

The micro-gap chamber

F. Angelini, R. Bellazzini, A. Brez, M.M. Massai, R. Raffo, G. Spandre and M.A. Spezziga

INFN-Pisa and University of Pisa, Via Livornese 582-I-56010 S. Piero a Grado, Pisa, Italy

Received 12 May 1993

The micro-gap chamber (MGC), a new type of position sensitive proportional gas counter, is introduced. The device is built using microelectronics technology. In this detector the separation between the electrodes collecting the avalanche charge (the anode–cathode gap) is only a few microns. The time it takes to collect the positive ions is therefore very short (≈ 10 ns). The speed of the device now equals that of solid state detectors but it is more than three orders of magnitude higher than in standard proportional counters and one order of magnitude higher than in the recently introduced microstrip gas chamber (MSGC). As a result, the rate capability is extremely high ($> 9 \times 10^6$ c/mm² s). The amplifying electric field around the thin anode microstrip extends over a small volume but is very intense (270 kV/mm). It provides a gas gain of 2.5×10^3 at 400 V with 14% (FWHM) energy resolution at 5.4 keV. The anode pitch is 100 μ m and the readout is intrinsically two-dimensional. Because there is practically no insulating material in view, charging was not observed even at the highest rate. This device seems very well suited for instrumentation of the tracking system at the new hadron colliders (LHC/SSC) as well as in many other fields of research.

1. Introduction

The introduction in the last few years of microelectronics technologies for the design and construction of modern gas detectors has led to a rejuvenation and a full renaissance of this class of detectors otherwise seriously challenged by other techniques for the instrumentation of the experiments at the new hadron colliders (LHC/SSC). The microstrip gas chamber (MSGC) is the clearest example of this process [1–4]. In a very short time this new device has been transformed from a laboratory curiosity into one of the building blocks of the inner tracking systems of almost all the proposed experiments at both LHC and SSC. This was due to very good detector performance, now very close to that of solid state microstrip detectors, as well as to its simplicity, low-cost and radiation resistance (intrinsic to a flushed detector with internal gas gain). Because of these features, the MSGC was implemented quickly to successfully track particles in two fixed target experiments at CERN, NA12 [5] and RD22 [6], clearly showing that it is already a useful instrument for present-day physics.

Nevertheless, it is well evident that we are just at the beginning of the exploitation of the enormous possibilities coming from the dramatic improvement in detector fabrication technology.

In this paper we report on the design, construction and test of a new device concept which could represent a further step forward in the field of gas detectors. The

most striking features of this new structure are the separation of only a few microns between the charge collecting electrodes (the anode–cathode gap) and the true possibility of an anode pitch ranging from 1 mm down to 50 μ m. The two aspects combine to provide performance in terms of speed as well as spatial and energy resolution which can hardly be matched by the other detectors based on the gas amplification of ionization electrons.

2. The detector

2.1. The detector internal structure

The new detector can be thought of as an ultra-miniaturized version of the multiwire proportional chamber (MWPC) [7] with highly asymmetric anode–cathode half-gaps. One half-gap has a standard thickness of 2–5 mm, the other has a thickness of only 2–4 μ m. The thick gap provides the primary ionization charge, while the ultrathin one is used to very quickly collect the positive charge created during the avalanche process. While in the MWPC the anodes float in the gas, in the micro-gap chamber (MGC) they are stuck onto a very thin insulating strip only a few microns wider than the anode microstrip itself. The electric field is set by the anode–cathode distance and it is substantially independent of the anode pitch which can

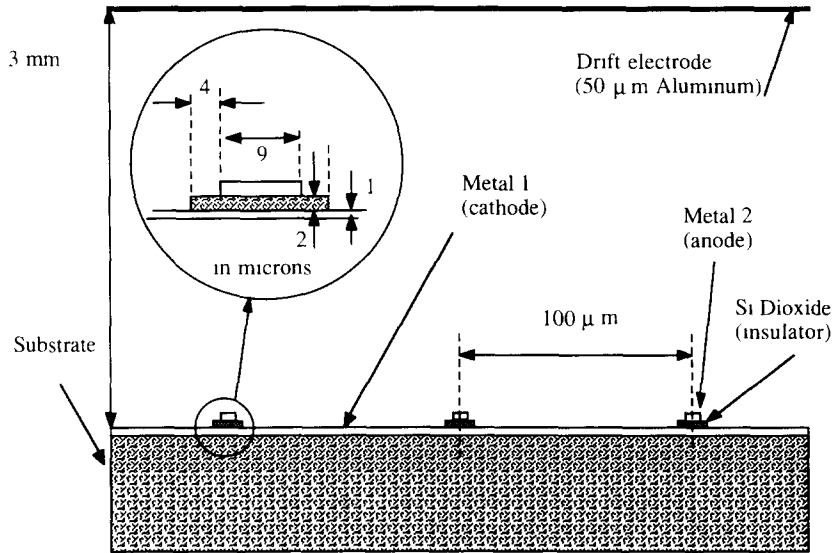


Fig. 1. A cross section of the detector internal structure.

therefore be freely chosen between 1 mm and 50 μm . Fig. 1 shows a cross section of the detector internal structure.

Moving from bottom to top we recognise:

i) the detector substrate (quartz), which acts only as a mechanical support. Any substrate material compatible with the silicon processing lines could be used as well (silicon, glass, sapphire, etc.). The present detectors have an area of $2.5\text{ cm} \times 2.5\text{ cm}$. Four different designs were integrated on a 4 in. wafer (500 μm

thick), but 6 and 8 in. are clearly possible. The substrate could be made much thinner (300 μm , for example) by back-grinding it at the end of the detector fabrication procedure. This is a standard technique in the microelectronics industry;

ii) the first aluminum film (metal 1, 1 μm thick) deposited onto the underlying quartz substrate. This metal layer is the positive charge collecting electrode (the cathode). The Al film was then patterned by standard photolithography and dry etching techniques

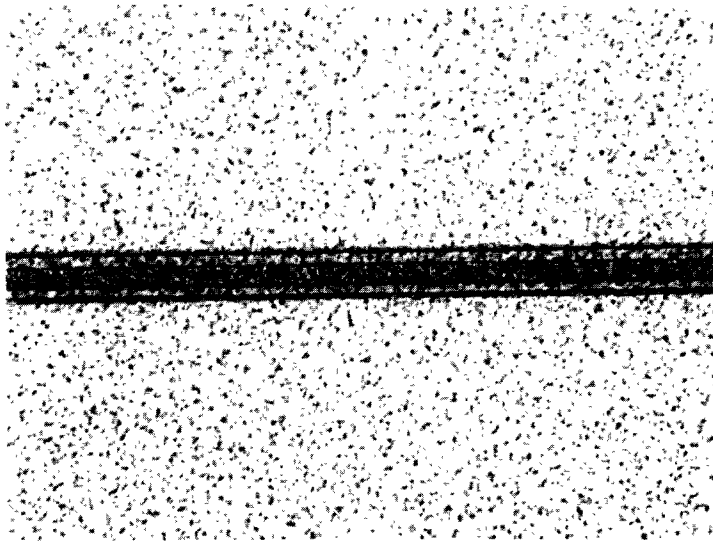


Fig. 2. A photograph of one anode-cathode micro-gap.

as wide (3.2 mm) strips to provide a coarse measurement of the coordinate along the anode strips (2D readout) or to provide the trigger;

iii) the 2 μm thick insulating strips obtained by patterning an intermetal oxide deposited on metal 1 by a plasma enhanced chemical vapour deposition technique (PECVD). These insulating strips set the anode-cathode distance and are only a few microns wider than the overlying anode microstrips. In this first run we have successfully tried oxide strips which are 8 μm wider (4 μm per side) than the anode strip. Because practically no insulating material is left exposed, charging of the substrate cannot occur and ion implantation of the oxide is not needed anymore;

iv) the second aluminum film (metal 2, 2 μm thick) deposited onto the oxide strips and on which the anode microstrips (5–9 μm wide, 100–200 μm apart) were engraved with a plasma etching technique. The anode microstrips lie on and run parallel to the oxide microstrip beneath. The side cathode strips of the MSGC do not exist anymore;

v) the gas gap (3 mm) which acts as active medium;

vi) the drift electrode that defines the collection region of the primary charge.

We have successfully operated also a 1D device which uses as substrate a low-resistivity silicon. The substrate itself acts, in this case, as the cathode.

A photograph of the anode-cathode micro-gap is shown in fig. 2.

2.2. The electrostatic field

To understand the operation of this device we have studied in detail the electric field configuration using a commercial electrostatic modeler (ELECTRO, I.E.S., Manitoba, Canada) which also includes dielectrics and resistive materials. For ease of comparison we have also studied the field configuration of a standard MWPC and of a standard MSGC.

Fig. 3 shows the field and the equipotential lines of the three detectors. The most striking feature of the MGC is the large number of field lines ending on the back cathode and the very steep voltage gradients. The electric field is much more intense in the MGC than in the MSGC and in the MWPC (by factors of 4 and 20, respectively). In such a configuration the ions created during the avalanche process will be collected very quickly at the near cathode and only a few per cent, if any, will be collected at the far drift cathode. The electric field is very intense, but extends over a small volume, so that the anode pitch does not affect the field down to 50 μm . Table 1 shows the anode capacitance for 50, 100 and 200 μm anode pitch and for several oxide thicknesses. The anode strip was assumed

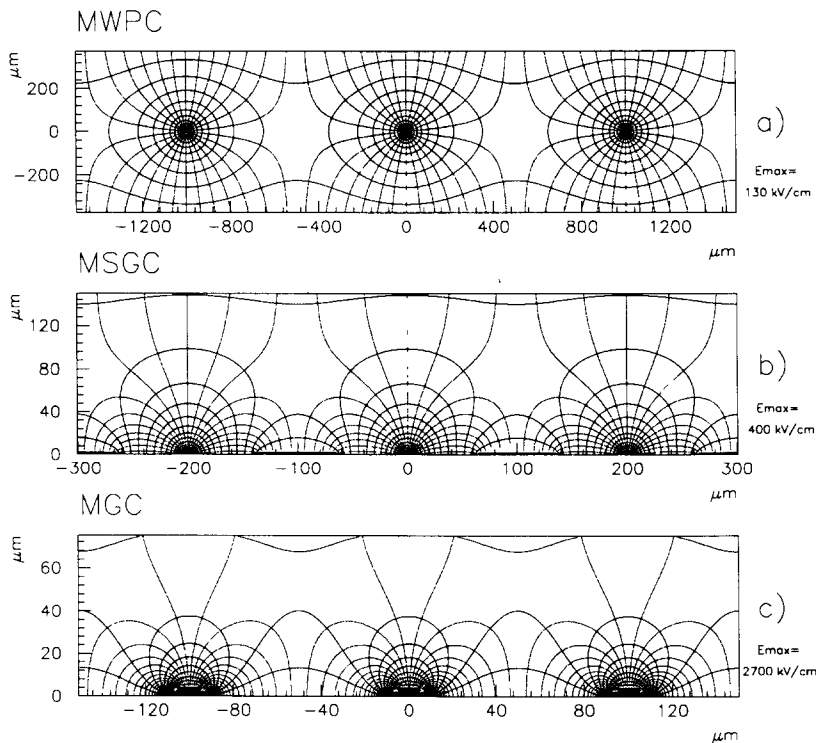


Fig. 3. Field and equipotential lines for a MWPC (a), for a MSGC (b) and for a MGC (c).

Table 1

The anode strip capacitance for three values of the thickness of the oxide strip and for 50, 100 and 200 μm anode pitch

Pitch [μm]	Thickness w [μm]	2 μm [pF/cm]	4 μm [pF/cm]	6 μm [pF/cm]
50	5	1.4	0.9	0.7
100	10	2.3	1.4	1
200	10	2.3	1.4	1

5 μm wide for the 50 μm pitch and 10 μm wide for the 100 and 200 μm anode pitch. The oxide strip was always 8 μm wider than the anode strip. The electrode capacitance is determined by the strip width and by the oxide thickness but does not depend on the pitch. Therefore, in the MGC for a fixed potential difference the gain is independent of the anode pitch. This has been confirmed experimentally for detectors with 100 and 200 μm anode distances which provided the same gain when the same potential was applied. The operation of the 100 μm pitch detector was as easy as for the 200 μm one.

2.3. The signal model

In the MGC the collection of the avalanche charge is very fast. Because the signal observed on the readout electrodes is induced by the separation of the charge carriers we expect the collection speed to have a large influence on the signal amplitude and on the signal time development. To study this quantitatively we have implemented the Gatti-Manfredi-Radeka [8,9] algorithm which models the process of current and charge induction on the detector electrodes. This model is based on Green's reciprocity theorem and computes the charge and current induced at any time on the electrodes by a point charge drifting toward the collecting electrode following the electrostatic field lines. Fig. 4 shows the main results for the MWPC, the MSGC and the MGC obtained assuming uniform avalanche charge distributions. More realistic distributions obtained by means of a full Monte Carlo simulation of the avalanche process will be implemented soon. If we take as a reference an electronics integration time of 20 ns we find that after this time the MWPC anode has delivered only 25% of the avalanche charge to the preamplifier, while the MSGC and the MGC anode strip have delivered 55% and 95% of their avalanche charges, respectively. In the MGC 90% of the charge is available after 10 ns only. This gas detector is as fast as a solid state device. For the cathodes we have, after 20 ns, a fraction of induced charge of 5% for the MWPC, 40% for the MSGC and 95% for the MGC. The difference between anode and cathode for the MWPC and MSGC is due to the charge in-

duced on the remaining electrodes (anode wires for the MWPC, anode and side cathode strips plus the back cathode for the MSGC). On the contrary, the MGC is a truly symmetric and two-dimensional device having anode and cathode signals with the same amplitude and time structure but opposite polarity.

From the simulated signal we have also extracted the information on the average time it takes for the full

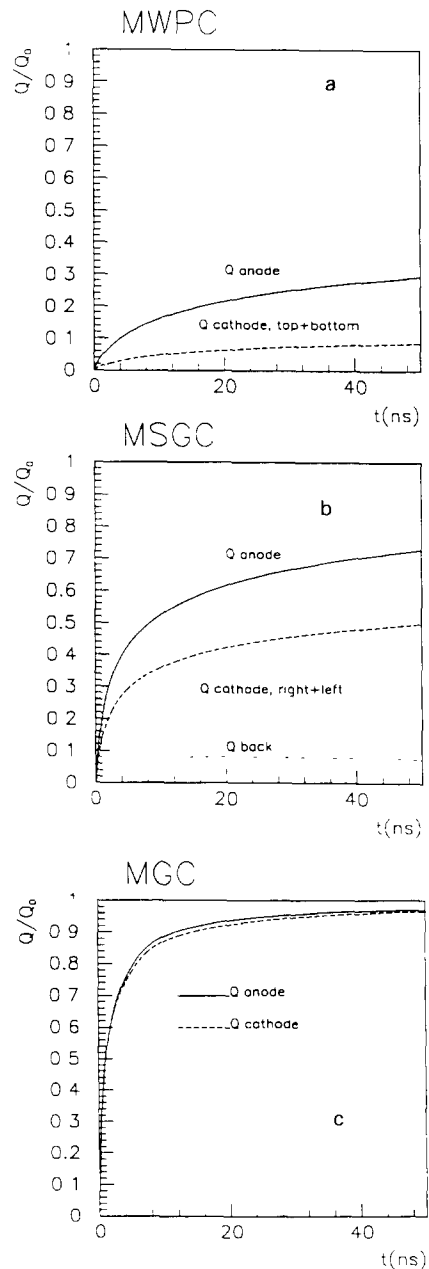


Fig. 4 Time development of the induced charge on the electrodes of a MWPC (a), a MSGC (b) and a MGC (c).

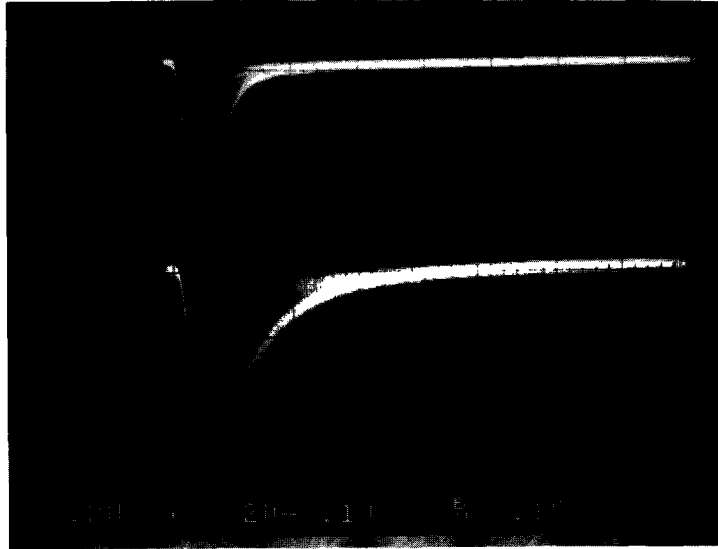


Fig. 5. The signal from the OR of two anode strips (upper trace) and the signal from the back cathode strip (lower trace) when the detector is illuminated with a ^{55}Fe source.

collection of the avalanche charge. This time affects the space charge buildup when working at very high rate. In the MWPC the ions are fully collected by the top and bottom cathodes in a rather low field. In the MGC the ions are almost all collected, if working at modest drift field ($\approx 1 \text{ kV/cm}$) by the very close back

cathode in a very intense field. For the MWPC we found a collection time of $84 \mu\text{s}$ and for the MGC of 9.2 ns . The MGC is, therefore, four orders of magnitude faster than the standard proportional counter. For the MSGC we found that the fraction of ions which go to the side cathodes is collected in 73 ns in

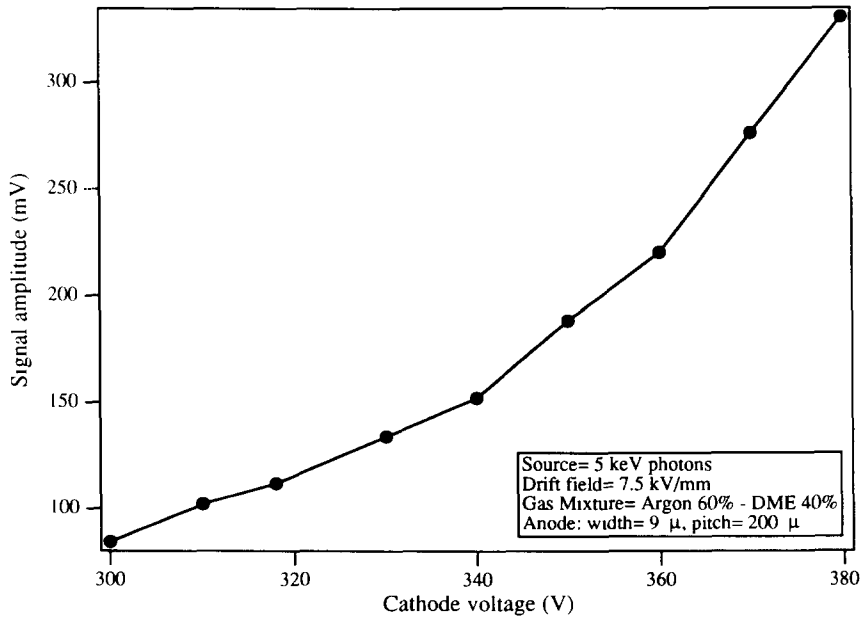


Fig. 6. Dependence of pulse-height on cathode potential.

average, while the fraction which drift to the front cathode is collected in 30 μs . The MGC is one order of magnitude faster than the MSGC.

3. The detector characteristics

3.1. The signals and the gain

All the results presented in this section refer to a device with 200 μm pitch, 9 μm wide anode strip and 17 μm wide oxide strip. Preliminary tests on 100 μm pitch devices have shown that these detectors work in a similar way. Detailed tests on these finer structures are still in progress in our laboratory.

Fig. 5 shows the signal from the OR of two anode strips (upper trace) together with the signal from the corresponding cathode strip (lower trace, inverted) which is hit when the 6 keV photons from ^{55}Fe source were collimated to a 2 mm² spot. Because the cathode strip is wider than the source, it collects the full charge from the photon conversion. The cathode signal has a well pronounced photopeak showing the very good proportionality of this detector. The large cathode strip capacitance (100 pF) affects strongly the signal/noise ratio, which is, obviously, much worse for the wide strip than for the anode strip. Furthermore, the RC product of the wide strip parallel capacitance and of its series resistance ($\approx 100 \Omega$) slows down the transfer of the charge collected by the pickup electrode to the input capacitance of the fast amplifier. Because of this ballistic deficit the cathode signal appears slower and smaller

than the anode signal but with the same area i.e. with the same charge. The use of thicker oxide or of more finely subdivided cathode readout will substantially improve both aspects. The cathode signals also show clearly the argon escape peak at 3 keV and the aluminum fluorescence line at 1.4 keV which is due to the aluminum entrance window. The photoelectric conversion in argon of a 1.4 keV photon provides 50 primary electrons which is roughly the charge released by a minimum ionizing particle in the thin detectors which have to be used at LHC/SSC.

The dependence of the pulse amplitude on the cathode voltage is reported in fig. 6. At 400 V the gas gain has been measured to be $\approx 2.5 \times 10^3$. It should be noted that if one works with a fast shaping time at the front-end electronics this gain corresponds in terms of integrated charge to $\approx 10^4$ for a MWPC and to $\approx 5 \times 10^3$ for a standard MSGC. The gas mixture was argon (60%)–DME (40%). This kind of detector needs a larger quenching fraction than the standard MSGC. This is clearly due to the close proximity of the cathode to the anode which calls for a corresponding reduction of the UV photons absorption mean free path to quench the avalanche. The potential difference of 400 V is 200 V lower than the one needed in the MSGC to have the same gain with the same gas mixture.

3.2. The energy resolution

In the micro-gap chamber the electric field is very high and limited to a rather small region around the anode strip. These conditions are supposed, according

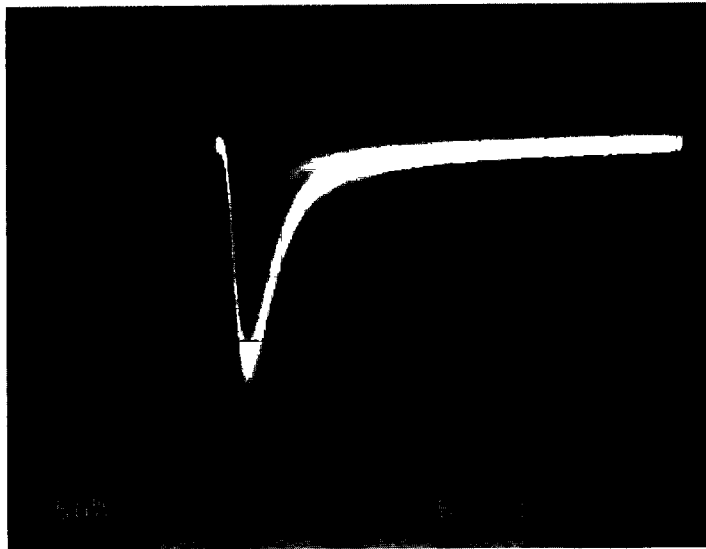


Fig. 7. The signal from the OR of several anode strips when the detector is illuminated with a Cr X-ray tube (5.4 keV line).

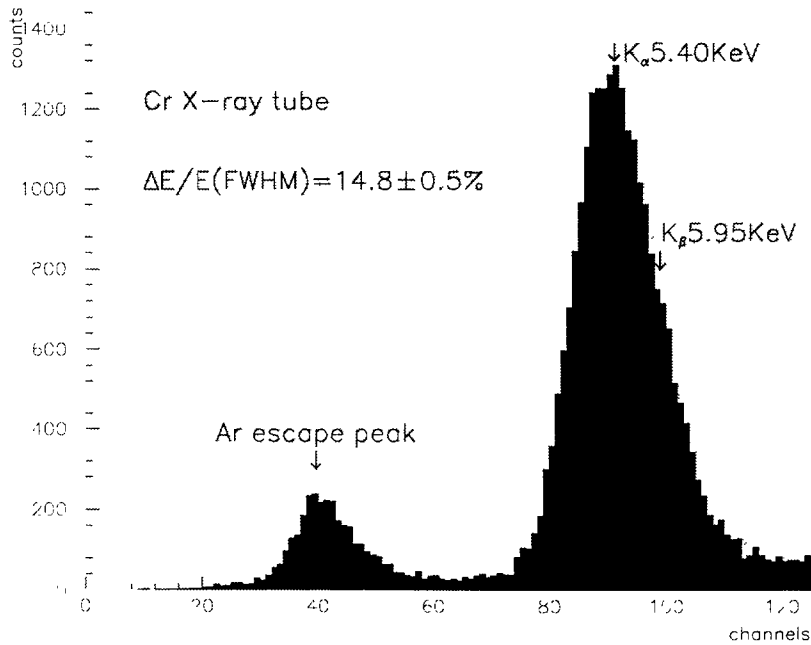


Fig. 8. The pulse-height spectrum of the signal of fig. 7.

to the well-established theory of Alkhozov [10], to favour low gain fluctuations and therefore good energy resolution.

We have studied the energy resolution of the MGC using the 5.4 keV chromium X-ray as a photon source, at a gas gain of 1500. Fig. 7 shows the signal observed with this source at an incident flux of 10^5 p/mm² s, while fig. 8 shows the corresponding pulse height spec-

trum. The resolution (FWHM) is 14.8% at 5.4 keV. The shoulder on the right side of the photopeak is due to the CrK_β line at 5.9 keV. We believe that this result, which is much better than what is obtained with the standard proportional counters, should be improved further by using slower, less noisy electronics, by using a different gas mixture (argon-ethane for example) and by working at a larger gain. It is interest-

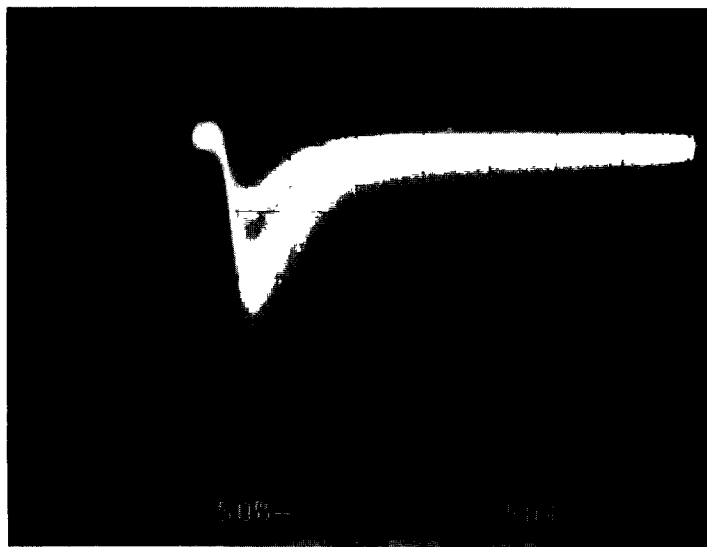


Fig. 9. The 5.4 keV signal from the OR of several anode strips at a flux of 2×10^6 p/mm² s.

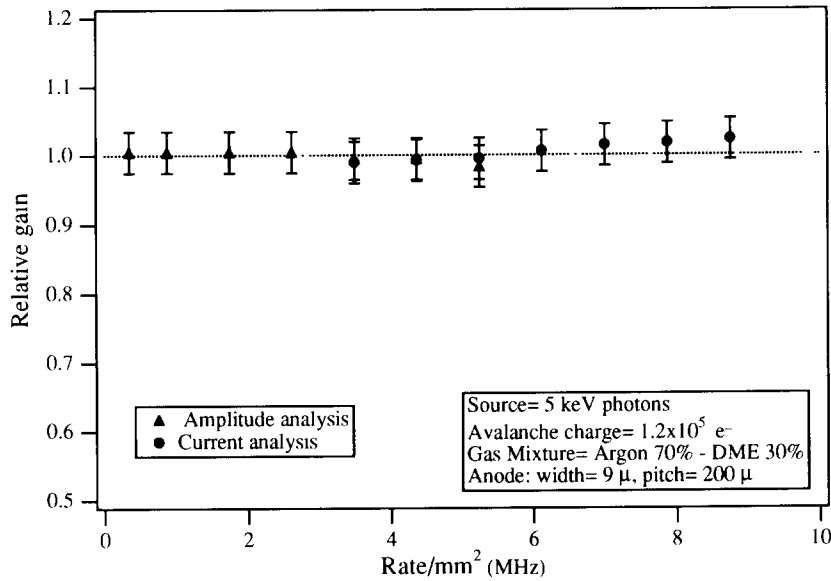


Fig. 10. The normalized gain as a function of rate.

ing to note that a good energy resolution is conserved even at very high rates as one can figure out from the signal shown in fig. 9. The incoming flux was, in this case, 2×10^6 p/mm² s.

3.3. The rate capability

The high charge collection speed and the fine pitch combine to give the MGC an extraordinary rate capability. The measurement of this performance has been

made with two different techniques. Between 10^5 and 10^6 p/mm² s we have looked at the stability of the signal pulse height as a function of rate using a Tektronix 2440 digital oscilloscope. Above this rate this kind of measurement starts to be biased by pileup problems. For this reason, between 10^6 and 10^7 p/mm² s we have looked at the stability of the signal current per unit flux as a function of flux. No dependence of gain on incoming flux has been observed up to flux of 9×10^6 p/mm² s (see fig. 10).

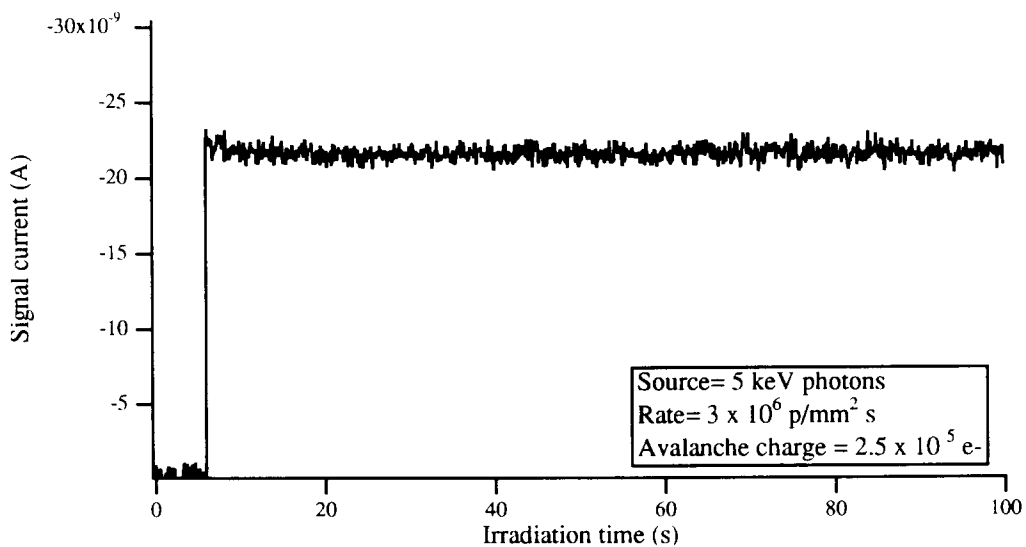


Fig. 11. The signal current as function of time for a point never irradiated before.

3.4. Charging

The MGC can be considered a dielectricless detector. Indeed, one of its essential features is the removal of practically all the insulating materials left exposed. From the technological point of view it is quite possible to have oxide strips only 2 μm wider than the anode strip. We have successfully used oxide strips 8 μm wider (4 μm per side) than the 9 μm overlying anode strip. In this way the charging problem is cured at the source and the ion implantation of the oxide or the use of low resistivity substrate is not needed anymore. Fig. 11 shows the signal current as a function of time when a point never irradiated before it was illuminated with the X -ray source. The incident flux was $3 \times 10^6 \text{ p/mm}^2 \text{ s}$ and the current sampling frequency was 10 Hz. No current drop could be observed.

An accelerated study of the ageing property of this new detector is planned for the near future.

4. Conclusions

A new position sensitive gas detector with very promising performance has been introduced. The speed of avalanche charge collection of this device is comparable with that of the solid state detectors.

The measured energy resolution (14.8% at 5.4 keV) and rate capability ($> 9 \times 10^6 \text{ p/mm}^2 \text{ s}$) and the expected position resolution put this detector in a separate class among the gas detectors.

The device has shown to be reasonably robust and reliable, even if a large improvement in this direction, together with an increase of gas gain, is expected after

the debugging of the detector design in the following runs.

The successful operation of this new concept is also a further demonstration of the enormous possibilities coming from the application of microelectronics technologies to the design and fabrication of gas detectors.

Finally, it is worth mentioning that such a detector with simple modifications of the readout organization could also find many interesting applications in different fields, such as astrophysics, synchrotron radiation and medical physics as an X -ray imaging device.

Acknowledgements

We thank G. Decarolis, M. Favati and C. Magazzu' of INFN-Pisa for their enthusiastic technical support.

References

- [1] A. Oed, Nucl. Instr. and Meth. A263 (1988) 351.
- [2] F. Angelini et al., Nucl. Instr. and Meth. A283 (1989) 755.
- [3] M.H.J. Gijsberts et al., Nucl. Instr. and Meth. A313 (1992) 377.
- [4] R. Bouclier et al., CERN-PPE/93-04.
- [5] F. Angelini et al., Nucl. Instr. and Meth. A315 (1992) 21.
- [6] RD22 Collaboration, CERN/DRDC 92-51.
- [7] G. Charpak et al., Nucl. Instr. and Meth. 62 (1968) 262.
- [8] E. Gatti and P.F. Manfredi, Riv. Nuovo Cimento 9 (1986).
- [9] V. Radeka, Ann. Rev. Nucl. Part. Sci. (1988) 217.
- [10] G.D. Alkhozov, Nucl. Instr. and Meth. 89 (1970) 155.